Jones matrix for image-rotation prisms

Ivan Moreno

The polarization-transforming properties of rotational prisms are analyzed with polarized light by using the Jones calculus and the exact ray-trace. A general expression of the Jones matrix for a rotational prism is derived, incorporating an explicit dependence on the image-rotation angle or the wave-front-rotation angle. The Jones matrix for the Pechan, Dove, Reversion, and Delta prisms is derived where the explicit dependence on the angle of rotation of the image is given. An experiment with a rotating Dove prism is also conducted to determine the output states of polarization for incident linearly polarized light. Experimental results agree with theoretical expectations. © 2004 Optical Society of America

OCIS codes: 230.5480, 080.2740, 350.4600, 260.5430.

1. Introduction

Rotational prisms are extensively used in optical instrumentation to rotate (or derotate) optical images by an arbitrary angle. A rotational prism causes inversion and rotation of the image that is equal to twice the angular mechanical rotation of the prism, while keeping the line of sight undeviated.[1–3] These optical properties indicate that rotational prisms can be key components within modern optical devices. In recent years, rotational prisms have been used in pattern-recognition systems,[4] interferometers,[5,6] the metrology of rotating objects,[7] optical profilers,[8] and optical parametric oscillators[9,10] and for measuring a rotational frequency shift.[11,12] However, rotational prisms have inherent polarization properties.

The polarization-transforming properties of rotational prisms are of particular interest because they influence the signal measurement of the optical instrument.[13,14] In image rotation an invariant signal is important when one intends to improve the resolution of the measurement, especially when the optical system is a polarization critical system. In optical design it is of interest to derive a practical expression of the Jones matrix for rotational prisms. This matrix must incorporate the explicit dependence on image-rotation angle. Such a matrix can be a compact and simple tool for quickly estimating the output state of polarization of light when images or wave fronts are rotated with a rotational prism.

In this paper we analyze the change in the state of polarization introduced by a rotational prism that rotates an optical image on polarized light. This is performed in Subsection 2.A with the Jones calculus and the exact ray-trace analysis. Subsection 2.B gives the Jones matrix for a general rotational prism that incorporates the explicit dependence on the angle of rotation of the image. The Jones matrix for the Pechan, Dove, Reversion, and Delta prisms is derived where the explicit dependence on the image-rotation angle is given (Sections 3–6). An experiment with a rotating Dove prism is also set up for determining the output states of polarization for incident linearly polarized light, confirming the theoretical analysis (Section 7). The conclusion is in Section 8.

2. Change in State of Polarization on Traversing Rotational Prisms

Our goal is to determine the state of polarization of a beam of light on passing through a rotated rotational prism. We consider the case of monochromatic illumination. To simplify the analysis, we consider the case of a polarized plane wave of light. We represent the coherent plane wave with a ray of light, incorporating the vector nature of this problem. An input ray undergoes an odd number of internal reflections on traversing a rotational prism.[15]

A. Three-Dimensional Polarization Ray Tracing

The polarization evaluation can be performed with the Jones matrices in three dimensions that transform the electric field along the wave-front path.[16–18] A rotational prism may be a prism assembly, in which case a polarization evaluation can be performed by

The author is with Facultad de Física, Universidad Autonoma de Zacatecas, Apdo. Postal C-580, 98060 Zacatecas, Zac., Mexico (e-mail, imoreno@planck.reduaz.mx).

Received 29 November 2003; revised manuscript received 9 March 2004; accepted 12 March 2004.

0003-6935/04/173373-09$15.00/0

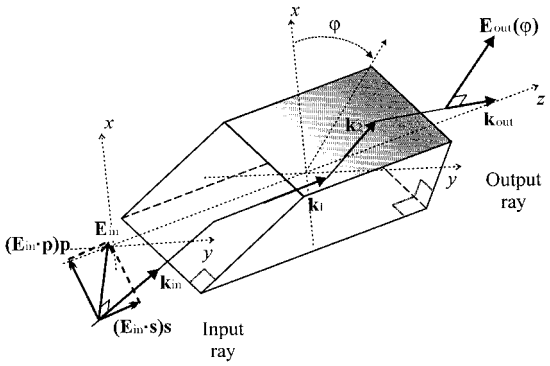

Fig. 1. Arbitrary propagation of polarized light through a simple rotational prism (Dove prism). The ray path is given by unit vectors $\mathbf{k}_{in}$, $\mathbf{k}_1$, $\mathbf{k}_2$, and $\mathbf{k}_{out}$.

using this analysis on each individual prism. We analyze a one-piece constructed prism. Polarization at the output of a rotational prism depends on the angle of the prism rotation with respect to the optical axis φ. The electric field at the output of a rotated rotational prism is

$$\mathbf{E}_{out}(\varphi) = \boldsymbol{\tau}_2\mathbf{r}_n, \ldots, \mathbf{r}_2\mathbf{r}_1\boldsymbol{\tau}_1\mathbf{E}_{in}, \tag{1}$$

where $\mathbf{E}_{in}$ is the electric field at the entrance to the rotational prism; $\boldsymbol{\tau}_1$ is the transmission matrix at the first refracting surface (input); $\mathbf{r}_n, \ldots, \mathbf{r}_1$ are the internal reflection matrices at each reflecting surface, where n is the number of internal reflections (an odd integer); and $\boldsymbol{\tau}_2$ is the transmission matrix at the last refracting surface (output). These matrices transform the state of polarization of the propagating beam. The polarization transformation depends on the ray path, whose direction is given by the unit vectors $\mathbf{k}_{in}, \mathbf{k}_1, \ldots, \mathbf{k}_{n+1}, \mathbf{k}_{out}$ (Fig. 1). Note that all the coefficients in all matrices depend on the prism index of refraction, the ray angle of incidence, and the angle of prism rotation.

We now present the transmission and the reflection matrices at each surface. In the matrix $\boldsymbol{\tau}_1$ the nondiagonal elements are different from zero because the normal vector of the first surface changes with the prism rotation. This change is with respect to the coordinate system of the input polarization state. Therefore there is a rotation between the two coordinate systems. This makes $\boldsymbol{\tau}_1$ equal to the matrix product of transmission and rotational matrices in a coordinate frame with respect to the ray path[17]:

$$\boldsymbol{\tau}_1 = \frac{1}{|\mathbf{k}_{in}\times\mathbf{n}_{in}|} \times \begin{bmatrix} t_{1\parallel}(\mathbf{k}_{in}\times\mathbf{n}_{in})\cdot\mathbf{s} & -t_{1\parallel}(\mathbf{k}_{in}\times\mathbf{n}_{in})\cdot\mathbf{p} \\ t_{1\perp}(\mathbf{k}_{in}\times\mathbf{n}_{in})\cdot\mathbf{p} & t_{1\perp}(\mathbf{k}_{in}\times\mathbf{n}_{in})\cdot\mathbf{s} \end{bmatrix}, \tag{2}$$

where $t_{1\parallel}$ and $t_{1\perp}$ are the Fresnel transmission coefficients at the entrance surface for the fields parallel and perpendicular to the plane of incidence, respectively. Unit vector $\mathbf{n}_{in}$ is normal to the entrance surface and oriented toward the exterior of the prism. Unit vectors $\mathbf{p}$ and $\mathbf{s}$ (which form an orthonormal basis with $\mathbf{k}_{in}$, the arbitrary direction of the incident wave front) form the vector basis of reference for describing the state of polarization of the entrance wave front. These unit vectors can be defined, for simplicity, as parallel $\mathbf{p}$ and normal $\mathbf{s}$ to the plane of incidence formed when the angle of prism rotation is zero.

The reflection matrix at the mth surface is

$$\mathbf{r}_m = \frac{1}{|\mathbf{k}_m\times\mathbf{n}_m||\mathbf{k}_m\times\mathbf{n}_{m-1}|}\begin{bmatrix} r_{m\parallel}(\mathbf{k}_m\times\mathbf{n}_m)\cdot(\mathbf{k}_m\times\mathbf{n}_{m-1}) & -r_{m\parallel}(\mathbf{k}_m\times\mathbf{n}_m)\cdot\mathbf{n}_{m-1} \\ r_{m\perp}(\mathbf{k}_m\times\mathbf{n}_m)\cdot\mathbf{n}_{m-1} & r_{m\perp}(\mathbf{k}_m\times\mathbf{n}_m)\cdot(\mathbf{k}_m\times\mathbf{n}_{m-1}) \end{bmatrix}, \tag{3}$$

where $r_{m\parallel}$ and $r_{m\perp}$ are the Fresnel reflection coefficients at the mth reflecting surface ($m = 1, 2, \ldots, n$) for fields parallel and perpendicular to the plane of incidence, respectively. The unit vector $\mathbf{n}_m$ is normal to the mth reflecting surface and oriented toward the interior of the prism (the unit vector $\mathbf{n}_0 = \mathbf{n}_{in}$). The incident wave front at the mth reflecting surface propagates along direction $\mathbf{k}_m$.

The transmission matrix at the output surface is

$$\boldsymbol{\tau}_2 = \frac{1}{|\mathbf{k}_{n+1}\times\mathbf{n}_{out}||\mathbf{k}_{n+1}\times\mathbf{n}_n|}\begin{bmatrix} t_{2\parallel}(\mathbf{k}_{n+1}\times\mathbf{n}_{out})\cdot(\mathbf{k}_{n+1}\times\mathbf{n}_n) & -t_{2\parallel}(\mathbf{k}_{n+1}\times\mathbf{n}_{out})\cdot\mathbf{n}_n \\ t_{2\perp}(\mathbf{k}_{n+1}\times\mathbf{n}_{out})\cdot\mathbf{n}_n & t_{2\perp}(\mathbf{k}_{n+1}\times\mathbf{n}_{out})\cdot(\mathbf{k}_{n+1}\times\mathbf{n}_n) \end{bmatrix}, \tag{4}$$

where $t_{2\parallel}$ and $t_{2\perp}$ are the Fresnel transmission coefficients at the exiting surface, parallel and perpendicular to the plane of incidence, respectively. Unit vector $\mathbf{n}_{out}$ is normal to the exiting surface and oriented toward the interior of the prism. The incident wave front at the output surface propagates along direction $\mathbf{k}_{n+1}$.

The polarization transformation depends on the rotation of the rotational prism, whose angle of rotation is introduced in unit vectors $\mathbf{n}_{in}, \mathbf{n}_1, \ldots, \mathbf{n}_n$, and $\mathbf{n}_{out}$. The exact ray trace includes these unit vectors

for calculating the unit direction vectors $\mathbf{k}_{\text{in}}$, $\mathbf{k}_1, \ldots,$ $\mathbf{k}_{n+1}$, and $\mathbf{k}_{\text{out}}$. The Fresnel coefficients at each prism surface are calculated with these ray-path vectors and surface-normal vectors.

B. Jones Matrix for Rotational Prisms

The Jones matrix for a rotational prism can be derived by incorporating the explicit dependence on the image-rotation angle 2φ. The polarization transformation depends on the ray path. We evaluate the Jones matrix for the case of the incident ray parallel to the optical axis (along the z direction). Then input and output unit base vectors can be chosen to be $\mathbf{i}$ and $\mathbf{j}$ (along the x and y directions). The Jones matrix for a rotational prism is the matrix product

$$\mathbf{T}(\varphi) = \mathbf{B}_{i,j}\mathbf{T}_N, \ldots, \mathbf{T}_1, \tag{5}$$

where $\mathbf{T}_N = \boldsymbol{\tau}_2\mathbf{r}_q, \ldots, \mathbf{r}_1\boldsymbol{\tau}_1$ is the Jones matrix for the Nth piece forming the prism assembly. On exiting the prism, the electric field is given in terms of vectors normal and parallel to the prism exit surface. However, this coordinate system changes with the prism rotation angle. Thus $\mathbf{B}_{i,j}$ is the matrix used to change the unit base vectors (relative to the plane of incidence at the output surface) of the electric field exiting the prism to those relative to the state of polarization of the entrance wave front ($\mathbf{i}$, $\mathbf{j}$):

$$\mathbf{B}_{i,j} = \begin{pmatrix} \cos\varphi & -\sin\varphi \\ \sin\varphi & \cos\varphi \end{pmatrix}. \tag{6}$$

This matrix corresponds to a simple rotation by angle φ of the coordinate system. The sign of the sine function in the diagonal elements corresponds to the negative rotation angle.

The matrix product in Eq. (5) may be evaluated in a straightforward manner to give the Jones matrix for a general rotational prism $\mathbf{T}(\varphi)$, where the explicit dependence on φ is given:

$$\mathbf{T}(\varphi) = \begin{bmatrix} -T_\parallel \cos^2\varphi - T_\perp \sin^2\varphi & (T_\perp - T_\parallel)\cos\varphi \sin\varphi \\ (T_\perp - T_\parallel)\cos\varphi \sin\varphi & -T_\parallel \sin^2\varphi - T_\perp \cos^2\varphi \end{bmatrix}, \tag{7}$$

where

$$T_\parallel = t_{1\parallel}t_{2\parallel}, \ldots, t_{2N\parallel}r_{1\parallel}r_{2\parallel}, \ldots, r_{n\parallel}, \tag{8}$$

$$T_\perp = t_{1\perp}t_{2\perp}, \ldots, t_{2N\perp}r_{1\perp}r_{2\perp}, \ldots, r_{n\perp}, \tag{9}$$

where $r_{1\parallel}, \ldots, r_{n\parallel}$ and $r_{1\perp}, \ldots, r_{n\perp}$ are the Fresnel reflection coefficients at each reflecting surface, where n is the number of internal reflections (an odd integer), for fields parallel and perpendicular to the plane of incidence, respectively. Coefficients $t_{1\parallel}, \ldots, t_{2N\parallel}$ and $t_{1\perp}, \ldots, t_{2N\perp}$ are the Fresnel transmission coefficients at each refractive surface (where N is the number of pieces forming the prism assembly) for the fields parallel and perpendicular to the plane of incidence, respectively. These Fresnel coefficients are constant with the prism-rotation angle because the incident ray is parallel to the optical axis.

The matrix $\mathbf{T}(\varphi)$ is the transformation of the electric field associated with the ray that crosses the rotational prism, rotated by angle φ. It transforms electric field $\mathbf{E}_{\text{in}}$ at the entrance to the rotational prism into electric field $\mathbf{E}_{\text{out}}(\varphi)$ at the exit of the rotated rotational prism:

$$\mathbf{E}_{\text{out}}(\varphi) = \mathbf{T}(\varphi)\mathbf{E}_{\text{in}}. \tag{10}$$

From this we can determine electric field $\mathbf{E}_{\text{out}}(\varphi)$, which is associated with the ray after it has exited the rotated rotational prism.

Matrix $\mathbf{T}(\varphi)$ is a practical expression of the Jones matrix for a general rotational prism that incorporates the explicit dependence on image-rotation angle 2φ. This matrix is a compact and simple tool that can be used to quickly estimate the output state of polarization of light when images or wave fronts are rotated with a rotational prism. The Jones matrices for the main rotational prisms are deduced below.

3. Jones Matrix for a Dove Prism

In terms of manufacturing requirements the most popular rotational prism is the Dove owing to its one-piece fabrication and absence of coatings. The ray path inside a Dove prism is the simplest. An input ray undergoes two refractions and one total internal reflection (TIR) on traversing a Dove prism. The Jones matrix for the Dove prism is the matrix product

$$\mathbf{T}(\varphi) = \mathbf{B}_{i,j}\boldsymbol{\tau}_2\mathbf{r}_1\boldsymbol{\tau}_1. \tag{11}$$

This matrix product is a particular case of the general expression in Eq. (7), which may be evaluated to give the Jones matrix for the Dove prism $\mathbf{T}(\varphi)$, where the explicit dependence on φ is given:

$$\mathbf{T}(\varphi) = \begin{bmatrix} -t_{1\parallel}t_{2\parallel}r_{1\parallel}\cos^2\varphi - t_{1\perp}t_{2\perp}r_{1\perp}\sin^2\varphi & (t_{1\perp}t_{2\perp}r_{1\perp} - t_{1\parallel}t_{2\parallel}r_{1\parallel})\cos\varphi \sin\varphi \\ (t_{1\perp}t_{2\perp}r_{1\perp} - t_{1\parallel}t_{2\parallel}r_{1\parallel})\cos\varphi \sin\varphi & -t_{1\parallel}t_{2\parallel}r_{1\parallel}\sin^2\varphi - t_{1\perp}t_{2\perp}r_{1\perp}\cos^2\varphi \end{bmatrix}, \tag{12}$$

where

$$\begin{aligned} T_\parallel &= t_{1\parallel}t_{2\parallel}r_{1\parallel} \\ &= \left\{\frac{(4n^2\sin\alpha)(n^2 - \cos^2\alpha)^{1/2}}{[n^2\sin\alpha + (n^2 - \cos^2\alpha)^{1/2}]^2}\right\} \\ &\quad \times \left\{\frac{\cos(\alpha + \alpha') - in[n^2\sin^2(\alpha + \alpha') - 1]^{1/2}}{\cos(\alpha + \alpha') + in[n^2\sin^2(\alpha + \alpha') - 1]^{1/2}}\right\}, \end{aligned} \tag{13}$$

$$T_{\perp} = t_{1\perp}t_{2\perp}r_{1\perp} = \left\{\frac{(4\ \sin\alpha)(n^2 - \cos^2\alpha)^{1/2}}{[\sin\alpha + (n^2 - \cos^2\alpha)^{1/2}]^2}\right\} \times \left\{\frac{n\ \cos(\alpha + \alpha') - i[n^2\ \sin^2(\alpha + \alpha') - 1]^{1/2}}{n\ \cos(\alpha + \alpha') + i[n^2\ \sin^2(\alpha + \alpha') - 1]^{1/2}}\right\}, \tag{14}$$

$$\alpha' = \arcsin\left(\frac{\cos\alpha}{n}\right). \tag{15}$$

Here α and n are the base angle and index of refraction of the Dove prism, respectively. The imaginary number i results from the TIR.

Figure 2 shows the calculated states of polarization at the output of a rotated Dove prism for different image rotation angles 2φ with linearly polarized light incident. The simulated prism is a Dove prism designed with a base angle of $\alpha = 45°$ and an optical glass of BK7 ($n = 1.515$ for $\lambda = 632.8$ nm). Although a Dove prism rotated by angle φ inverts and rotates an image by 2φ, the polarization plane is not rotated. The output electric field is only mildly elliptically polarized. The ellipse semimajor axis remains nearly parallel to the input plane of polarization, and its magnitude is appreciably larger than that of the minor axis. The sense of the elliptical polarization is in the same direction as that of the prism rotation when the image rotates from 0 to ± 180 deg. The maximum polarization change occurs at ± 90 deg image rotation, as shown in Fig. 2(b).

4. Jones Matrix for a Delta Prism

In terms of compactness requirements the smallest rotational prism is the Delta because of its triangular geometry. An input ray undergoes two refractions and three internal reflections on traversing a Delta prism. The TIR occurs in sequence at the exit and the entrance faces. The intermediate face must be aluminized to make it reflective. The Jones matrix for the Delta prism is the matrix product:

$$\mathbf{T}(\varphi) = \mathbf{B}_{i,j}\boldsymbol{\tau}_2\mathbf{r}_3\mathbf{r}_2\mathbf{r}_1\boldsymbol{\tau}_1. \tag{16}$$

This matrix product is a particular case of the general expression in Eq. (7), which may be evaluated to give the Jones matrix for the Delta prism $\mathbf{T}(\varphi)$, where the explicit dependence on φ is given:

$$\mathbf{T}(\varphi) = \begin{bmatrix} -t_{1\parallel}t_{2\parallel}r_{1\parallel}r_{2\parallel}r_{3\parallel}\cos^2\varphi - t_{1\perp}t_{2\perp}r_{1\perp}r_{2\perp}r_{3\perp}\sin^2\varphi & (t_{1\perp}t_{2\perp}r_{1\perp}r_{2\perp}r_{3\perp} - t_{1\parallel}t_{2\parallel}r_{1\parallel}r_{2\parallel}r_{3\parallel})\cos\varphi\sin\varphi \\ (t_{1\perp}t_{2\perp}r_{1\perp}r_{2\perp}r_{3\perp} - t_{1\parallel}t_{2\parallel}r_{1\parallel}r_{2\parallel}r_{3\parallel})\cos\varphi\sin\varphi & -t_{1\parallel}t_{2\parallel}r_{1\parallel}r_{2\parallel}r_{3\parallel}\sin^2\varphi - t_{1\perp}t_{2\perp}r_{1\perp}r_{2\perp}r_{3\perp}\cos^2\varphi \end{bmatrix}, \tag{17}$$

where

$$T_{\parallel} = t_{1\parallel}t_{2\parallel}r_{1\parallel}r_{2\parallel}r_{3\parallel} = \left\{\frac{(4n^2\cos\theta)(n^2 - \sin^2\theta)^{1/2}}{[n^2\cos\theta + (n^2 - \sin^2\theta)^{1/2}]^2}\right\} \times \left\{\frac{\cos(2\theta - \theta') - in[n^2\sin^2(2\theta - \theta') - 1]^{1/2}}{\cos(2\theta - \theta') + in[n^2\sin^2(2\theta - \theta') - 1]^{1/2}}\right\}^2 \times \left\{\frac{n_M{}^2\sin(3\theta - \theta') - n[n_M{}^2 - n^2\cos^2(3\theta - \theta')]^{1/2}}{n_M{}^2\sin(3\theta - \theta') + n[n_M{}^2 - n^2\cos^2(3\theta - \theta')]^{1/2}}\right\}, \tag{18}$$

$$T_{\perp} = t_{1\perp}t_{2\perp}r_{1\perp}r_{2\perp}r_{3\perp} = \left\{\frac{(4\cos\theta)(n^2 - \sin^2\theta)^{1/2}}{[\cos\theta + (n^2 - \sin^2\theta)^{1/2}]^2}\right\} \times \left\{\frac{n\cos(2\theta - \theta') - i[n^2\sin^2(2\theta - \theta') - 1]^{1/2}}{n\cos(2\theta - \theta') + i[n^2\sin^2(2\theta - \theta') - 1]^{1/2}}\right\}^2 \times \left\{\frac{n\sin(3\theta - \theta') - [n_M{}^2 - n^2\cos^2(3\theta - \theta')]^{1/2}}{n\sin(3\theta - \theta') + [n_M{}^2 - n^2\cos^2(3\theta - \theta')]^{1/2}}\right\}, \tag{19}$$

$$\theta' = \arcsin\left(\frac{\sin\theta}{n}\right), \tag{20}$$

where 2θ is the apex angle of the prism, n is the index of refraction of the prism, and n_M is the complex index of refraction of the metal deposited on the intermediate surface. The imaginary number i results from the TIR.

Figure 3 shows the calculated states of polarization at the output of a rotated Delta prism for different image rotation angles 2φ. The simulated prism is a Delta prism designed with apex angle $2\theta = 60°$ and optical glass SF11 ($n = 1.785$ for $\lambda = 546$ nm) and $n_M = 0.82 - i5.99$ (aluminum film at $\lambda = 546$ nm). In the design of a Delta prism a glass with a high index of refraction is necessary to reduce the required apex angle for TIR occurrence.

Although a Delta prism rotated by angle φ inverts and rotates an image by 2φ, the polarization plane is not rotated. The output electric field is elliptically polarized. The sense of the elliptical polarization is contrary to that of the prism rotation when the image rotates from 0 to ± 180 deg. The maximum polarization change occurs at a ± 90-deg image rotation, as shown in Fig. 3(b).

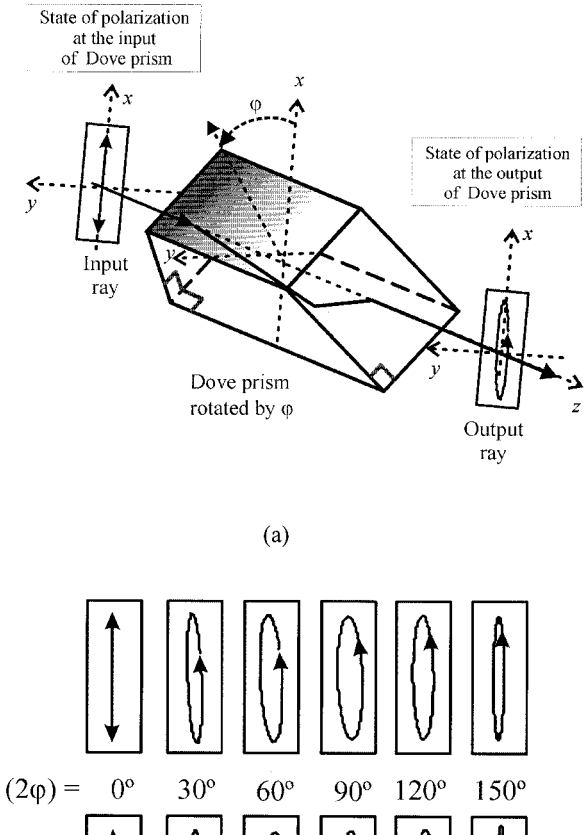

Fig. 2. Calculated polarization states at the output of a rotated Dove prism. The simulated prism is a Dove prism designed with a base angle of $\alpha = 45°$ and optical glass BK7 ($n = 1.515$ for $\lambda = 632.8$ nm). (a) Dove prism rotated by angle φ with linearly polarized incident light. (b) State of polarization at the output of a Dove prism for different image-rotation angles 2φ. (The Dove prism is rotated by φ.) The output state of polarization is mildly elliptically polarized.

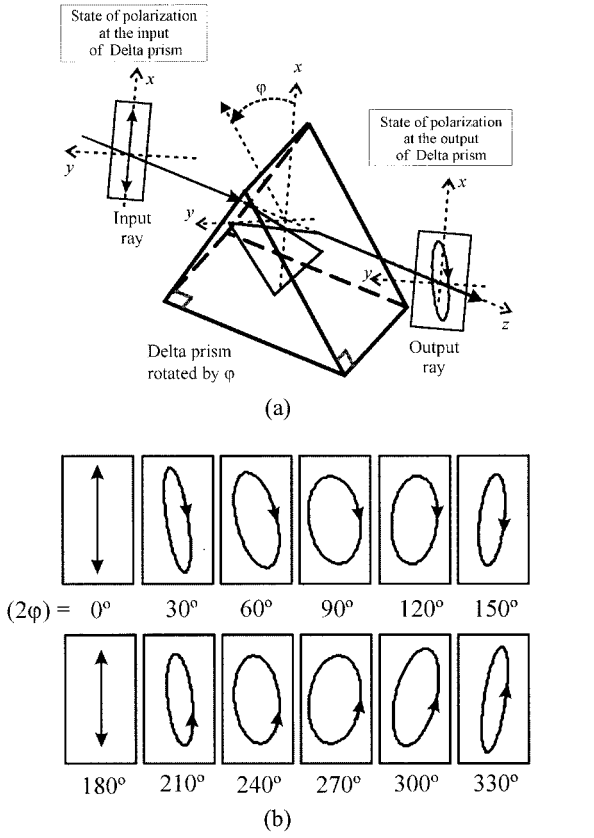

Fig. 3. Calculated polarization states at the output of a rotated Delta prism. The simulated prism is a Delta prism designed with an apex angle of $2\theta = 60°$ and optical glass SF11 ($n = 1.785$ for $\lambda = 546$ nm) and $n_M = 0.82 - i5.99$ (aluminum film at $\lambda = 546$ nm). (a) Delta prism rotated by angle φ with linearly polarized incident light. (b) State of polarization at the output of a Delta prism for different image-rotation angles 2φ. (The Delta prism is rotated by φ.) The output state of polarization is elliptically polarized.

5. Jones Matrix for a Reversion Prism

The Reversion prism, also called the roofless Abbe or K prism, is a two-component (cemented) prism. It is an image rotator just like the Dove and Delta prisms, but it can be used in converging or diverging beams of light. An input ray undergoes four refractions and three internal reflections on traversing a Reversion prism. The intermediate face must be aluminized to make it reflective. TIR occurs at the first and the last reflecting surfaces. The Jones matrix for the Reversion prism is the matrix product

$$\mathbf{T}(\varphi) = \mathbf{B}_{i,j}\boldsymbol{\tau}_4\mathbf{r}_3\boldsymbol{\tau}_3\boldsymbol{\tau}_2\mathbf{r}_2\mathbf{r}_1\boldsymbol{\tau}_1. \tag{21}$$

This matrix product is a particular case of the general expression in Eq. (7), which may be evaluated to give the Jones matrix for the Reversion prism $\mathbf{T}(\varphi)$, where the explicit dependence on φ is given:

$$\mathbf{T}(\varphi) = \begin{bmatrix} -t_1t_2t_3t_4(r_{1\parallel}r_{2\parallel}r_{3\parallel}\cos^2\varphi + r_{1\perp}r_{2\perp}r_{3\perp}\sin^2\varphi) & t_1t_2t_3t_4(r_{1\perp}r_{2\perp}r_{3\perp} - r_{1\parallel}r_{2\parallel}r_{3\parallel})\cos\varphi\sin\varphi \\ t_1t_2t_3t_4(r_{1\perp}r_{2\perp}r_{3\perp} - r_{1\parallel}r_{2\parallel}r_{3\parallel})\cos\varphi\sin\varphi & -t_1t_2t_3t_4(r_{1\parallel}r_{2\parallel}r_{3\parallel}\sin^2\varphi + r_{1\perp}r_{2\perp}r_{3\perp}\cos^2\varphi) \end{bmatrix}, \tag{22}$$

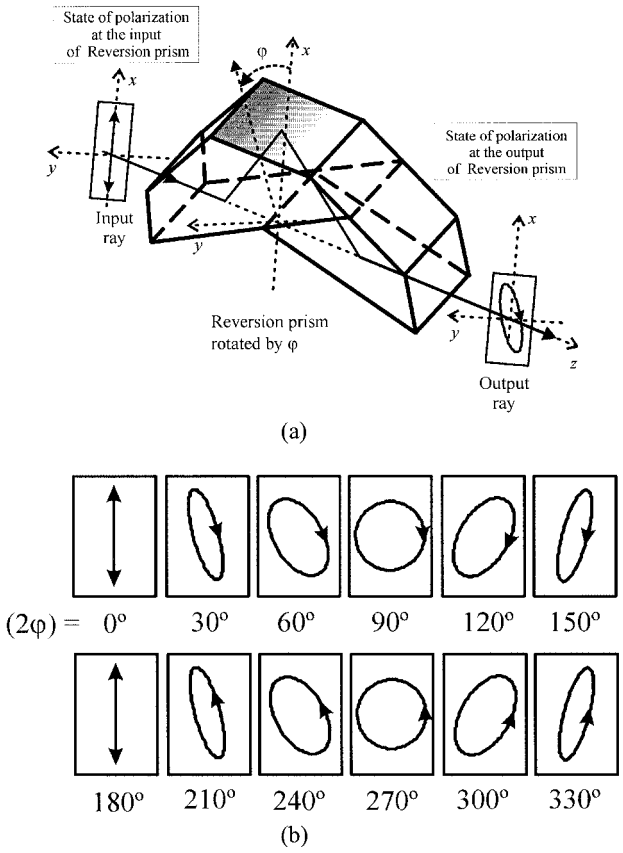

Fig. 4. Calculated polarization states at the output of a rotated Reversion prism. The simulated prism is a Reversion prism designed with optical glass BK7 ($n = 1.519$ for $\lambda = 546$ nm) with $n_M = 0.82 - i5.99$ (aluminum film at $\lambda = 546$ nm) and a typical optical cement of $n_c = 1.53$. (a) Reversion prism rotated by an angle φ with linearly polarized light incident. (b) State of polarization at the output of the Reversion prism for different image-rotation angles 2φ. (The Reversion prism is rotated by φ.) The output state of polarization is strongly elliptically polarized.

where

$$T_{\parallel} = t_1 t_2 t_3 t_4 r_{1\parallel} r_{2\parallel} r_{3\parallel} = \left(\frac{2\sqrt{n}}{n+1}\right)^2 \left[\frac{2(nn_c)^{1/2}}{n+n_c}\right]^2 \left[\frac{1 - in(3n^2-4)^{1/2}}{1 + in(3n^2-4)^{1/2}}\right]^2 \times \left[\frac{\sqrt{3}n_M^2 - n(4n_M^2 - n^2)^{1/2}}{\sqrt{3}n_M^2 + n(4n_M^2 - n^2)^{1/2}}\right], \quad (23)$$

$$T_{\perp} = t_1 t_2 t_3 t_4 r_{1\perp} r_{2\perp} r_{3\perp} = \left(\frac{2\sqrt{n}}{n+1}\right)^2 \left[\frac{2(nn_c)^{1/2}}{n+n_c}\right]^2 \left[\frac{n - i(3n^2-4)^{1/2}}{n + i(3n^2-4)^{1/2}}\right]^2 \times \left[\frac{\sqrt{3}n - (4n_M^2 - n^2)^{1/2}}{\sqrt{3}n + (4n_M^2 - n^2)^{1/2}}\right], \quad (24)$$

where n is the index of refraction of the prism, n_c is the index of refraction of the optical cement, and n_M is the complex index of refraction of the metal deposited on the intermediate surface. The imaginary number i results from the TIR.

Figure 4 shows the calculated states of polarization at the output of a Reversion prism for different image-rotation angles 2φ with linearly polarized incident light. The simulated prism is a Reversion prism designed with optical glass BK7 ($n = 1.519$ for $\lambda = 546$ nm) with $n_M = 0.82–i5.99$ (aluminum film at $\lambda = 546$ nm) and typical optical cement of $n_c = 1.53$.

Although a Reversion prism rotated by angle φ inverts and rotates an image by 2φ, the polarization plane is not rotated. The output electric field is strongly elliptically polarized. The sense of the elliptical polarization is inverse to that of the prism rotation when the image rotates from 0 to ± 180 deg. The maximum polarization change occurs at a ± 90-deg image rotation, as shown in Fig. 4(b). The light becomes circularly polarized at ± 90 deg of image rotation in the special case of the prism considered with the above parameters.

6. Jones Matrix for a Pechan Prism

The Pechan prism is a compact two-component prism used in converging or diverging beams. The two parts are usually held together mechanically to create a narrow air space between them, permitting TIR to occur. An input ray undergoes four refractions and five internal reflections on traversing a Pechan prism. The two outer reflecting faces must be aluminized. The TIR occurs at the first and the third reflection. The Jones matrix for the Pechan prism is the matrix product:

$$\mathbf{T}(\varphi) = \mathbf{B}_{i,j}\boldsymbol{\tau}_4\mathbf{r}_5\mathbf{r}_4\mathbf{r}_3\boldsymbol{\tau}_3\boldsymbol{\tau}_2\mathbf{r}_2\mathbf{r}_1\boldsymbol{\tau}_1. \quad (25)$$

This matrix product is a particular case of the general expression in Eq. (7), which may be evaluated to give the Jones matrix for the Pechan prism $\mathbf{T}(\varphi)$, where an explicit dependence on φ is given:

$$\mathbf{T}(\varphi) = \begin{bmatrix} t_1 t_2 t_3 t_4 (r_{1\parallel} r_{2\parallel} r_{3\parallel} r_{4\parallel} r_{5\parallel} \cos^2\varphi + r_{1\perp} r_{2\perp} r_{3\perp} r_{4\perp} r_{5\perp} \sin^2\varphi) & -t_1 t_2 t_3 t_4 (r_{1\perp} r_{2\perp} r_{3\perp} r_{4\perp} r_{5\perp} - r_{1\parallel} r_{2\parallel} r_{3\parallel} r_{4\parallel} r_{5\parallel}) \cos\varphi \sin\varphi \\ -t_1 t_2 t_3 t_4 (r_{1\perp} r_{2\perp} r_{3\perp} r_{4\perp} r_{5\perp} - r_{1\parallel} r_{2\parallel} r_{3\parallel} r_{4\parallel} r_{5\parallel}) \cos\varphi \sin\varphi & t_1 t_2 t_3 t_4 (r_{1\parallel} r_{2\parallel} r_{3\parallel} r_{4\parallel} r_{5\parallel} \sin^2\varphi + r_{1\perp} r_{2\perp} r_{3\perp} r_{4\perp} r_{5\perp} \cos^2\varphi) \end{bmatrix}, \quad (26)$$

where

$$T_{\parallel} = t_1 t_2 t_3 t_4 r_{1\parallel} r_{2\parallel} r_{3\parallel} r_{4\parallel} r_{5\parallel} = \left(\frac{2\sqrt{n}}{n+1}\right)^4 \left[\frac{1 - in(n^2-2)^{1/2}}{1 + in\sqrt{n^2-2}}\right]^3 \times \left[\frac{n_M{}^2 \cos\frac{\pi}{8} - n\left(n_M{}^2 - n^2 \sin^2\frac{\pi}{8}\right)^{1/2}}{n_M{}^2 \cos\frac{\pi}{8} + n\left(n_M{}^2 - n^2 \sin^2\frac{\pi}{8}\right)^{1/2}}\right]^2, \quad (27)$$

$$T_{\perp} = t_1 t_2 t_3 t_4 r_{1\perp} r_{2\perp} r_{3\perp} r_{4\perp} r_{5\perp} = \left(\frac{2\sqrt{n}}{n+1}\right)^4 \left[\frac{n - i(n^2-2)^{1/2}}{n + i(n^2-2)^{1/2}}\right]^3 \times \left[\frac{n_M \cos\frac{\pi}{8} - \left(n_M{}^2 - n^2 \sin^2\frac{\pi}{8}\right)^{1/2}}{n_M \cos\frac{\pi}{8} + \left(n_M{}^2 - n^2 \sin^2\frac{\pi}{8}\right)^{1/2}}\right]^2, \quad (28)$$

where n is the index of refraction of the prism and n_M is the complex index of refraction of the metal deposited on the aluminized surfaces. The imaginary number i results from the TIR.

Figure 5 shows the calculated states of polarization at the output of a Pechan prism for different image rotation angles 2φ with linearly polarized incident light. The simulated prism is a Pechan prism designed with optical glass BK7 ($n = 1.515$ for $\lambda = 632.8$ nm) and $n_M = 1.44 + i5.23$ (aluminum film at $\lambda = 632.8$ nm).

A Pechan prism rotated by an angle φ inverts and rotates an image by 2φ, and the polarization plane is rotated by φ. Then the Pechan prism behaves like a linear polarizer. The output electric field is linearly polarized with its amplitude modulated. The sense of the polarization rotation is in the same direction as that of the prism rotation, when the image rotates from 0 to ± 360 deg. The maximum polarization change occurs at a ± 180-deg image rotation, where the electric field is zero, as shown in Fig. 5(b).

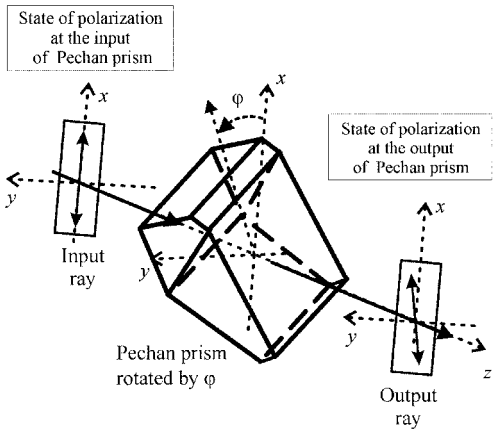

(a)

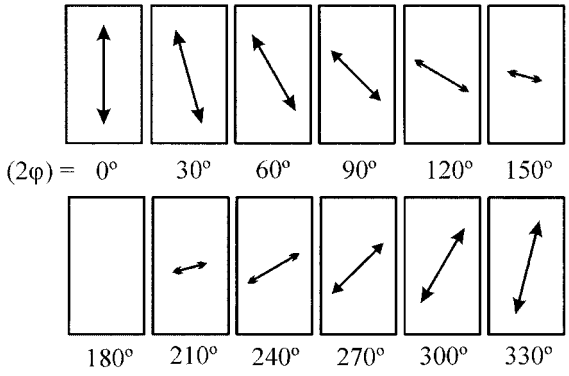

(b)

Fig. 5. Calculated polarization states at the output of a rotated Pechan prism. The simulated prism is a Pechan prism designed with optical glass BK7 ($n = 1.515$ for $\lambda = 632.8$ nm) and $n_M = 1.44 + i5.23$ (aluminum film at $\lambda = 632.8$ nm). (a) Pechan prism rotated by angle φ with linearly polarized incident light. (b) State of polarization at the output of a Pechan prism for different image-rotation angles 2φ. (The Pechan prism is rotated by φ.) The output state of polarization is linearly polarized, and the polarization plane is rotated by φ.

7. Experimental Confirmation

We performed an experiment to confirm the validity of the theoretical work. A Dove prism made of BK7 ($n = 1.515$ for $\lambda = 632.8$ nm), with $45° \pm 5$-arc min angle, is analyzed. Its aperture diameter is 20.00 ± 0.13 mm, and its length is 81.30 ± 0.38 mm. Its coatings. Its surface accuracy is estimated at 1λ, whereas the surface quality is approximately 60/40. We evaluate the Jones matrix, Eq. (12), for this case, obtaining the following values for the matrix $\mathbf{T}(\varphi)$:

$$\mathbf{T}(\varphi) = \begin{bmatrix} (0.9244 - 0.3568i)\cos^2\varphi + (0.6248 - 0.6539i)\sin^2\varphi & (0.2996 + 0.2971i)\cos\varphi\sin\varphi \\ (0.2996 + 0.2971i)\cos\varphi\sin\varphi & (0.9244 - 0.3568i)\sin^2\varphi + (0.6248 - 0.6539i)\cos^2\varphi \end{bmatrix}. \quad (29)$$

internal absorption is estimated at $A = 0.011$. Only Fresnel losses, already incorporated into the Jones matrix, are anticipated because of the absence of The experiment to confirm the theoretical analysis is described below. A beam of light emitted from a He–Ne laser of 632.8-nm wavelength passes through

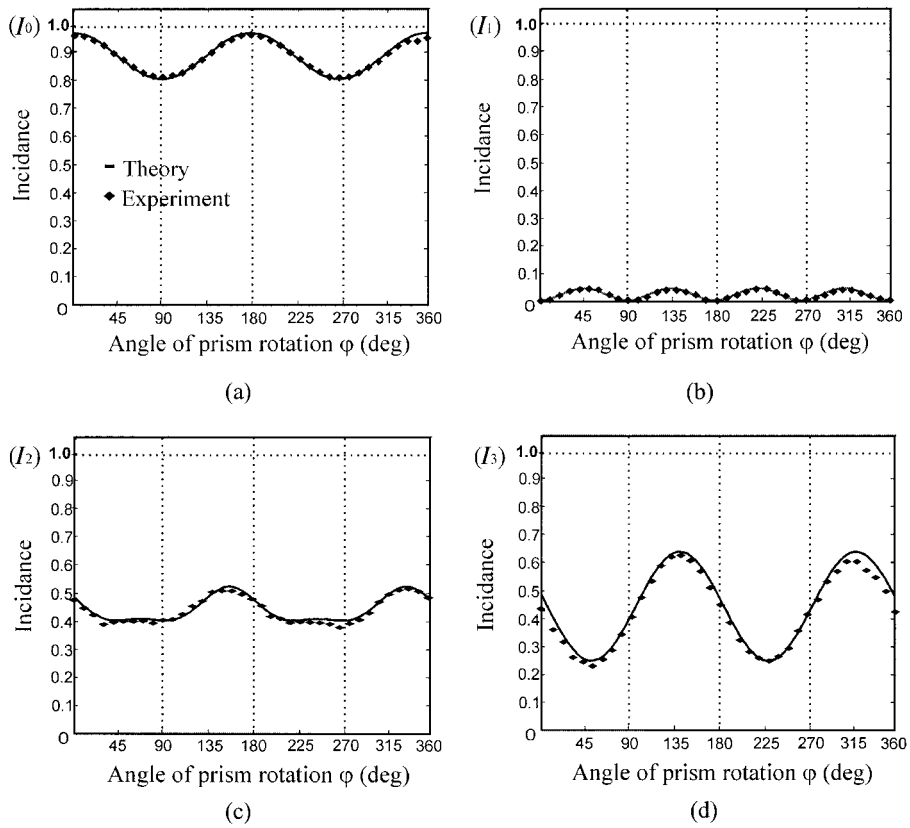

Fig. 6. Comparison between the theoretical and the experimental results for incidances I_0, I_1, I_2, and I_3 at the output of the Dove prism as a function of the prism angle of rotation φ. These are the incidance measurements of the beam transmitted through the filters corresponding to the Stokes parameters. (a) The first filter is isotropic, passing all states equally and transmitting light with incidance I_0. (b) The second filter is a linear polarizer with the horizontal transmission axis (i.e., along the y direction) transmitting I_1. (c) The third is a linear polarizer with the transmission axis at +45°, transmitting I_2. (d) The fourth filter is a circular polarizer opaque to left-circularly polarized light, transmitting I_3.

the Dove prism. Using linear polarizers and a $\lambda/4$ retarder plate, we measure the transmitted incidances[19] associated with the Stokes parameters[20] of the electric field at the output of a rotated Dove prism. In our reference system the incident linear polarization is along the x direction (vertical). Linearly polarized light passes through the Dove prism, rotated by successively larger angles, in increments of 10 deg. Thus measurements of incidance are performed as a function of prism rotation angle φ in increments of an angle of $\Delta\varphi = 10$ deg. Incidance is measured at the output, after the beam has passed through a filter associated with each Stokes parameter. Each set of measurements is performed with one of four different filters: an isotropic filter, a linear polarizer with a horizontal axis, a linear polarizer with an axis at 45°, and a circular polarizer opaque to left-circularly polarized light.

The theoretically predicted values are confirmed in the measurements. Simulated incidances are calculated with the square modulus of the output electric field and are normalized with respect to the incidance at the prism entrance pupil of the prism ($I_{\text{in}} \propto |\mathbf{E}_{\text{in}}|^2$). The normalized incidance of the beam transmitted through the isotropic filter (the one that transmits all states equally) is

$$I_0(\varphi) = \frac{|\mathbf{E}_{\text{out}}(\varphi)|^2}{|\mathbf{E}_{\text{in}}|^2}, \tag{30}$$

where $\mathbf{E}_{\text{out}}(\varphi)$ is the output electric field, determined from Eq. (10) and the Jones matrix of Eq. (29).

The normalized incidance of the light transmitted through the second filter (i.e., a linear polarizer with the horizontal transmission axis along the y direction) is

$$I_1(\varphi) = \frac{|\mathbf{J}_y\mathbf{E}_{\text{out}}(\varphi)|^2}{|\mathbf{E}_{\text{in}}|^2}, \tag{31}$$

where $\mathbf{J}_y$ is the Jones matrix of a linear polarizer with the transmission axis along the y direction (horizontal).

The normalized incidance of the transmitted light through the third filter (i.e., a linear polarizer with the transmission axis at +45°) is

$$I_2(\varphi) = \frac{|\mathbf{J}_{+45}\mathbf{E}_{\text{out}}(\varphi)|^2}{|\mathbf{E}_{\text{in}}|^2}, \tag{32}$$

where $\mathbf{J}_{+45}$ is the Jones matrix of a linear polarizer with the transmission axis at +45°.

The normalized incidence of the transmitted light through the fourth filter, a circular polarizer opaque to left-circularly polarized light (we implemented the circular polarizer with a $\lambda/4$ retarder plate and a +45° polarizer), is

$$I_3(\varphi) = \frac{|\mathbf{J}_{+45}\mathbf{J}_{\lambda/4}\mathbf{E}_{\text{out}}(\varphi)|^2}{|\mathbf{E}_{\text{in}}|^2}, \tag{33}$$

where $\mathbf{J}_{\lambda/4}$ is the Jones matrix of a $\lambda/4$ plate whose fast axis[21] is along the x direction (vertical).

Figure 6 shows that the experimental results agree with the theoretical predictions. It shows the quantities in Eqs. (30)–(33), when the incident light is polarized along the vertical direction (the x axis), $\mathbf{E}_{\text{in}} = |\mathbf{E}_{\text{in}}|\mathbf{i}$. A comparison between the theoretical and the experimental results for normalized incidances I_0, I_1, I_2, and I_3 at the output of the Dove prism as a function of the prism angle of rotation φ is shown. The first filter is isotropic, passing all states equally and transmitting light with incidance I_0 [see Fig. 6(a)]. In Fig. 6(b) the filter is a linear polarizer with the horizontal transmission axis (i.e., along the y direction) transmitting I_1. The third is a linear polarizer with the transmission axis at +45°, transmitting I_2 [see Fig. 6(c)]. The fourth filter is a circular polarizer opaque to left-circularly polarized light, transmitting I_3 [as shown in Fig. 6(d)].

The experimental results agree with the theoretical expectations. The slight discrepancy, especially in Figs. 6(c) and 6(d), is explained by the fact that the measurement requires careful orientation and alignment of polarizers and the $\lambda/4$ retarder plate. Additionally, the polarizers do not fully polarize the light, and a small portion of unpolarized light is transmitted. In summary, this experiment provides validation for the above analysis and the Jones matrix derived for image-rotation prisms.

8. Conclusions

We have applied the theory of the Jones calculus and the vector ray trace to analyze with polarized light the polarization-transforming properties of rotational prisms. We have derived a practical expression of the Jones matrix for a generalized rotational prism, incorporating an explicit dependence on the image-rotation angle. This matrix is a compact and simple tool that can be used to quickly estimate the output state of the polarization of light when images or wave fronts are rotated with a rotational prism. The Jones matrix for the Pechan, Dove, Reversion, and Delta prisms has been derived, where the explicit dependence on image-rotation angle is given. Using these matrices, we have displayed graphically for several image-rotation angles the transformation of the polarization state at the output of these prisms. An experiment with a rotating Dove prism has been performed to determine the output states of polarization for incident linearly polarized light. Experimental results have confirmed the theoretical expectations.

References

1. W. L. Wolfe, "Nondispersive prisms," in *Handbook of Optics*, 2nd ed., M. Bass, E. W. Van Stryland, D. R. Williams, and W. L. Wolfe, eds. (McGraw-Hill, New York, 1995), pp. 4.1–4.29.
2. D. L. Sullivan, "Alignment of rotational prisms," Appl. Opt. **11,** 2028–2032 (1972).
3. P. R. Yoder, Jr., *Design and Mounting of Prisms and Small Mirrors in Optical Instruments* (SPIE Press, Bellingham, Wash., 1998), Vol. TT32, pp. 19–57.
4. H. Fujii and Y. Ohtsuka, "Rotational filtering for randomly oriented pattern recognition," Opt. Commun. **36,** 255–257 (1981).
5. I. Moreno, G. Paez, and M. Strojnik, "Dove prism with increased throughput for implementation in a rotational-shearing interferometer," Appl. Opt. **42,** 4514–4521 (2003).
6. M. Strojnik Scholl and G. Paez, "Simulated interferometric patterns generated by a nearby star-planet system and detected by a rotational shearing interferometer," J. Opt. Soc. Am. A **16,** 2019–2024 (1999).
7. C. Perez-Lopez, F. Mendoza Santoyo, G. Pedrini, S. Schedin, and H. J. Tiziani, "Pulsed digital holographic interferometry for dynamic measurement of rotating objects with an optical derotator," Appl. Opt. **40,** 5106–5110 (2001).
8. P. Z. Takacs, E. L. Church, C. J. Bresloff, and L. Assoufid, "Improvements in the accuracy and the repeatability of long trace profiler measurements," Appl. Opt. **38,** 5468–5479 (1999).
9. A. V. Smith and M. S. Bowers, "Image-rotating cavity designs for improved beam quality in nanosecond optical parametric oscillators," J. Opt. Soc. Am. B **18,** 706–713 (2001).
10. D. J. Armstrong and A. V. Smith, "Demonstration of improved beam quality in an image-rotating optical parametric oscillator," Opt. Lett. **27,** 40–42 (2002).
11. J. Leach, M. J. Padgett, S. M. Barnett, S. Franke-Arnold, and J. Courtial, "Measuring the orbital angular momentum of a single photon," Phys. Rev. Lett. **88,** 257901 (2002).
12. J. Courtial, K. Dholakia, D. A. Robertson, L. Allen, and M. J. Padgett, "Measurement of the rotational frequency shift imparted to a rotating light beam possessing orbital angular momentum," Phys. Rev. Lett. **80,** 3217–3219 (1998).
13. I. Moreno, P. Velasquez, C. R. Fernandez-Pousa, and M. M. Sanchez-Lopez, "Jones matrix method for predicting and optimizing the optical modulation properties of a liquid-crystal display," J. Appl. Phys. **94,** 3697–3702 (2003).
14. M. J. Padgett and J. P. Lesso, "Dove prisms and polarized light," J. Mod. Opt. **46,** 175–179 (1999).
15. E. J. Galvez and C. D. Holmes, "Geometric phase of optical rotators," J. Opt. Soc. Am. A **16,** 1981–1985 (1999).
16. R. A. Chipman, "Mechanics of polarization ray tracing," Opt. Eng. **34,** 1636–1645 (1995).
17. E. Waluschka, "Polarization ray trace," Opt. Eng. **28,** 86–89 (1989).
18. M. Strojnik Scholl, "Ray trace through a corner-cube retroreflector with complex reflection coefficients," J. Opt. Soc. Am. A **12,** 1589–1592 (1995).
19. M. Strojnik and G. Paez, "Radiometry," in *Handbook of Optical Engineering*, D. Malacara and B. Thompson, eds. (Marcel Dekker, New York, 2001), Chap. 18, pp. 649–699.
20. W. A. Shurcliff, *Polarized Light* (Harvard University, Cambridge, Mass., 1957).
21. J. M. Bennett, "Polarization," in *Handbook of Optics*, 2nd ed., M. Bass, E. W. Van Stryland, D. R. Williams, and W. L. Wolfe, eds. (McGraw-Hill, New York, 1995), p. 5.1.